Transition Met Chem (2011) 36:433–439
DOI 10.1007/s11243-011-9487-x

An α-Diimine-Nickel(II) catalyst bearing an electron-withdrawing substituent for olefin polymerization

**Jianchao Yuan · Xuehu Wang · Tongjian Mei ·
Yufeng Liu · Chengping Miao · Xiaoli Xie**

Received: 24 January 2011 / Accepted: 21 March 2011 / Published online: 6 April 2011

Abstract A Br-substituted α-diimine ligand, bis[N,N′-(4-bromo-2,6-dimethylphenyl)imino]-2,3-butadiene **L1**, and its corresponding Ni(II) complex, {bis[N,N′-(4-bromo-2,6-dimethylphenyl)imino]-2,3-butadiene} dibromonicke **[$NiBr_2$(L1)]**, have been synthesized and characterized. The crystal structure of the free ligand (**L1**) was determined by X-ray crystallography. Two α-diimine-Ni(II) catalysts, {bis[N,N′-(2,4,6-dimethylphenyl)imino]-2,3-butanedione} dibromonickel **[$NiBr_2$(L2)]** and {bis[N,N′-(2,6-dimethylphenyl)imino]-2,3-butanedione} dibromonickel **[$NiBr_2$(L3)],** were also synthesized and characterized for comparison. The complex **[$NiBr_2$(L1)]**, when activated by diethylaluminum chloride, produces the most active catalytic system for the polymerization of ethylene among the three complexes. NMR analysis shows that the degree of branching of polyethylene increases in the presence of electron-withdrawing groups under the same reaction conditions.

Introduction

A major focus of our work has involved the development of olefin polymerization catalysts based upon α-diimine complexes of Ni(II) or Pd(II), the first report of which appeared in 1995 by Brookhart and coworkers [1]. The development of late-transition-metal catalysts for the polymerization of olefins has been spurred by their potential to yield polymers with different microstructures and also the need for catalysts that are more tolerant of functionalized monomers [2–12].

The catalyst activity and properties of the resulting polymers are greatly dependent on the reaction conditions [13–15] and ligand structure [16–18]. For a given catalyst, increasing the polymerization temperature increases the branching content of the polymer [19–23]. This effect is usually related to the competition between the chain walking and chain propagation processes. To gain more insight into the factors controlling the activity of such catalysts and the effect of catalyst structure on polymer structure and properties, the steric effects of the ortho substituent of the 2,6-dialkylaryl imine group on the catalytic activity of α-diimine-Ni(II) complexes has been studied in detail by Brookhart [6]. However, the effects of *para* substituents of the 2,6-dialkylaryl imine group [24, 25], especially of electron-withdrawing substituents, on the catalytic behavior of α-diimine-Ni(II) complexes and the properties of the resulting polymers has only been reported in limited cases [3].

In this work, we carried out an investigation into the catalytic behavior of three Ni(II) α-diimine catalysts activated by diethylaluminum chloride (DEAC). In this paper, we describe the effects of different substituents at the *para*-position of the 2,6-dialkylaryl imine group on the catalyst activity and polymer properties.

Experimental

All manipulations involving air- and/or water-sensitive compounds were carried out with standard Schlenk techniques using magnetic stirring under argon or nitrogen. Toluene and methylene chloride were distilled from

---

J. Yuan (✉) · X. Wang · T. Mei · Y. Liu · C. Miao · X. Xie
Key Laboratory of Eco-Environment-Related Polymer Materials,
Ministry of Education, Key Laboratory of Polymer Materials
of Gansu Province, College of Chemistry and Chemical
Engineering, Northwest Normal University,
Lanzhou 730070, China
e-mail: jianchaoyuan@nwnu.edu.cn

sodium/benzophenone under dry nitrogen. O-dichlorobenzene was dried over phosphorus pentoxide for 24 h, and then distilled under nitrogen. DEAC (0.9 mol/L solution in toluene) was purchased from Acros Organics. DME (1,2-dimethoxyethane) was distilled under N_2 from sodium. Anhydrous $NiBr_2$ (99%) was obtained from Aldrich. 2,3-Butanedione, 2,6-dimethylaniline (98%), 2,4,6-trimethylaniline (98%), and 4-bromo-2,6-dimethylaniline (98%) were purchased from Alfa Aesar and used without further purification. [$NiBr_2$(DME)] was synthesized according to the literature [26].

NMR spectra were recorded at 400 (^{13}C) and 100 (^{1}H) MHz, respectively, on a Varian Mercury plus-400 instrument, using TMS as internal standard. FTIR spectra were recorded on a Digilab Merlin FTS 3000 FTIR spectrophotometer on KBr pellets. X-ray photoelectron spectra (XPS) were obtained from a PHI-5702 multifunction instrument. The molecular weights and polydispersities (PDI) of the polymers were determined via an Alliance GPCV2000 (Waters) gel permeation chromatograph (GPC) using 1,2,4-trichlorobenzene as the eluent at a flow rate of 1.0 mL/min and operated at 140 °C.

Polymerization procedure

The polymerization was carried out in a 250-mL Schlenk flask equipped with a magnetic stirrer. The flask was repeatedly evacuated and refilled with nitrogen and finally filled with ethylene gas (ambient pressure). DEAC and toluene (50 mL) were added into the reactor. Ethylene was introduced under 0.02 Mpa until the solution was saturated and the pressure was maintained throughout each run. The reactor was evacuated, pressurized with ethylene, and then placed in an oil bath set at the operating temperature, and allowed to equilibrate for 10–15 min. The catalyst was dissolved in o-dichlorobenzene under dry nitrogen, and the solution was transferred into the Schlenk flask to initiate the polymerization. After 30 min at the desired temperature, the polymerization was stopped by turning the ethylene off and relieving the pressure. The reaction mixture was poured into a 2% HCl–MeOH solution to precipitate the polymer. The polymer was isolated by filtration, washed with methanol, and dried under vacuum.

Synthesis of bis [N, N′-(4-bromo-2,6-dimethylphenyl) imino]-2,3-butadiene (**L1**)

Formic acid (0.5 ml) was added to a stirred solution of 2,3-butanedione (0.260 g, 3 mmol) and 4-bromo-2,6-dimethylaniline (1.224 g, 6 mmol) in ethanol (20 ml). The mixture was refluxed for 24 h, then cooled, and the precipitate was filtered off. The solid was recrystallized from EtOH/CH_2Cl_2 (v/v = 8:1), washed with cold ethanol, and dried under vacuum. Yield: 1.22 g (82%). ^{1}H NMR (400 MHz, $CDCl_3$): δ 2.02 (s, 12H, Ar–CH_3), 2.35 (s, 6H, CCH_3), 7.26 (s, 4H, Ar–*H*). ^{13}C NMR (100 MHz, $CDCl_3$): δ 15.91 (C–CH_3), 17.61 (Ar–CH_3), 115.85 (Ar–*C*–Br), 126.88 (Ar–*C*), 130.56 (Ar–*C*–CH_3), 147.22 (Ar–*C*–N), and 168.50 (*C*=N). FTIR (KBr) 1,642 cm^{-1} (C=N). Anal. Calc. for $C_{20}H_{22}N_2Br_2$: C, 53.36; H, 4.93; N, 6.22. Found: C, 53.38; H, 4.92; N, 6.21.

Synthesis of bis [N, N′-(2, 4, 6-trimethylphenyl) imino]-2,3-butadiene (**L2**)

Formic acid (0.5 ml) was added to a stirred solution of 2,3-butanedione (0.260 g, 3 mmol) and 2,4,6-trimethylaniline (0.812 g, 6 mmol) in ethanol (20 mL). The mixture was stirred at 45 °C for 24 h, then cooled, and the precipitate was filtered off. The solid was recrystallized from EtOH/CH_2Cl_2 (v/v = 10:1), washed with cold ethanol, and dried under vacuum. Yield: 0.91 g (85%). ^{1}H NMR (400 MHz, $CDCl_3$): δ 2.00 (s, 12H, Ar–*o*–CH_3), 2.03 (s, 6H, Ar–*p*–CH_3), 2.29 (s, 6H, CCH_3), 6.89 (s, 4H, Ar–*H*). ^{13}C NMR (100 MHz, $CDCl_3$): δ 15.77 (C–CH_3), 17.70 (Ar–*o*–CH_3), 20.70 (Ar–*p*–CH_3), 124.52 (Ar–*C*), 128.55 (Ar–*C*–o–CH_3), 132.37 (Ar–*C*–p–CH_3), 145.86 (Ar–*C*–N), 168.32 (*C*=N). FT-IR (KBr) 1,637 cm^{-1} (C=N). Anal. Calc. for $C_{22}H_{28}N_2$: C, 82.45; H, 8.81; N, 8.74. Found: C, 82.50; H, 8.85; N, 8.64.

Synthesis of bis [N, N′-(2, 6-dimethylphenyl) imino]-2, 3-butadiene (**L3**)

Formic acid (0.5 ml) was added to a stirred solution of 2,3-butanedione (0.346 g, 4 mmol) and 2,6-dimethylaniline (0.970 g, 8 mmol) in ethanol (30 ml). The mixture was stirred at 45 °C for 24 h, then cooled, and the precipitate was filtered off. The solid was recrystallized from EtOH/CH_2Cl_2 (v/v = 10:1), washed with cold ethanol, and dried under vacuum. Yield: 1.16 g (88%). ^{1}H NMR (400 MHz, $CDCl_3$): δ 2.00 (s, 12H, Ar–CH_3), 2.35 (s, 6H, CCH_3), 6.96 (s, 4H, Ar–CH_3–*p*–*H*), 7.08 (s, 2H, Ar–CH_3–*m*–*H*). ^{13}C NMR (100 MHz, $CDCl_3$): δ 15.80 (C–CH_3), 17.78 (Ar–CH_3), 123.22 (Ar–*C*–m–CH_3), 124.63 (Ar–*C*–o–CH_3), 127.90 (Ar–*C*–CH_3), 148.30 (Ar–*C*–N), 168.03 (*C*=N). FT-IR (KBr) 1,637 cm^{-1} (C=N). Anal. Calc. for $C_{20}H_{24}N_2$: C, 82.15; H, 8.27; N, 9.58. Found: C, 82.20; H, 8.23; N, 8.63.

Synthesis of **[$NiBr_2$(L1)]**

[$NiBr_2$(DME)] (0.615 g, 2 mmol) was added to a stirred solution of **L1** (0.894 g, 2 mmol) in dichloromethane (30 ml). The mixture was stirred at room temperature for 18 h. The resulting suspension was filtered. The solvent was removed under vacuum and the residue was washed with diethyl ether (3·16 ml) and dried under vacuum. Yield 1.21 g (80%). Anal. Calc. (%) for $C_{20}H_{22}Br_4NiN_2$: C, 35.92; H, 3.32; N, 4.19. Found: C, 38.05; H, 3.84; N, 3.89. FT-IR (KBr) 1,639 cm^{-1} (C=N).

Synthesis of **$[NiBr_2(L2)]$**

$[NiBr_2(DME)]$ (0.615 g, 2 mmol) was added to a stirred solution of **L2** (0.643 g, 2 mmol) in dichloromethane (30 ml). The mixed was stirred for 18 h under nitrogen. The solution was filtered, and the filtrate was evaporated to dryness. The residue was washed with diethyl ether (3·16 mL) and dried under vacuum. Yield 1.07 g (85%). Anal. Calc. (%) for $C_{22}H_{28}Br_2NiN_2$: C, 49.03; H, 5.24; N, 5.20. Found: C, 49.11; H, 5.40; N, 5.25. FT-IR (KBr) 1,628 cm^{-1} (C=N).

Synthesis of **$[NiBr_2(L3)]$**

$[NiBr_2(DME)]$ (0.615 g, 2 mmol) was added to a stirred solution of **L3** (0.584 g, 2 mmol) in dichloromethane (30 ml). The mixer was stirred for 18 h under nitrogen. The solution was filtered, and the solvent was evaporated to dryness. The residue was washed with diethyl ether (3·16 mL) and dried under vacuum. Yield 0.99 g (83%). Anal. Calc. (%) for $C_{20}H_{24}Br_2NiN_2$: C, 47.02; H, 4.73; N, 5.48. Found: C, 49.20; H, 4.80; N, 5.50. FT-IR (KBr) 1,628 cm^{-1} (C=N).

X-ray crystallography

Crystals of **L1** suitable for X-ray analysis were obtained at room temperature by dissolving the ligand in CH_2Cl_2, following by slow layering of the solution with pentane.

X-ray diffraction data were collected on a Bruker APEX diffractometer equipped with a normal focus, 2.4 kW sealed tube X-ray source (Mo$K\alpha$ radiation, $\lambda = 0.71073$ Å) operating at 50 kV and 30 mA. The structure was solved by direct methods using SHELXS-97 and refined by full-matrix least-squares techniques with SHELXL-97. Crystal data, data collection, and refinement parameters are listed in Table 1.

Table 1 Crystal data and structure refinement for α-diimine ligand **L1**

Empirical formula	$C_{20} H_{22} Br_2 N_2$
Formula weight	450.22
Crystal system	Monoclinic
Space group	I2/a
Temperature	296(2) K
a(Å)	16.335(16)
b(Å)	7.376(7)
c(Å)	16.89(3)
α(°)	90 deg
β(°)	90.977(7) deg
γ(°)	90 deg
Volume	2,035(4) $Å^3$
Z	4
Calculated density	1.470 mg/m^3
Crystal size (mm)	0.30 × 0.28 × 0.21
F(000)	904
Theta range for data	2.49–25.50 deg.
Reflections collected	4,582
Unique	1,829 [*R*(int) = 0.0428]
Max and min transmission	0.4881 and 0.3809
Limiting indices	−19 <= h <= 19, −8 <= k <= 6, −19 <= l <= 20
Data/restraints/parameters	1,829/0/112
Refinement method	Full-matrix least-squares on F^2
Goodness-of-fit on F^2	1.094
Final *R* indices [$I > 2sigma(I)$]	$R_1 = 0.0531$, $wR_2 = 0.1503$
R indices (all data)	$R_1 = 0.1163$, $wR_2 = 0.1766$
Largest diff. peak and hole	0.311 and −0.517 $e.A^{-3}$

Crystallographic date for the structure has been deposited at the Cambridge Crystallographic Data Centre, CCDC 800153, deposition @ccdc.cam.ac.uk, http://www.ccdc.cam.ac.uk/deposit, Telephone: (44) 01223 762910, Facsimile: (44) 01223 336033, Postal Address: CCDC,12 Union Road, CAMBRIDGE CB2 1EZ, UK

Results and discussion

The general synthetic route to these nickel(II) complexes is shown in Scheme 1. The free ligands **L1–L3** were prepared by the condensation of two equivalents of the appropriate aniline with one equivalent of 2,3-butanedione, usually in the presence of an acid catalyst. The corresponding α-diimine Ni(II) complexes were synthesized in good yields by treating $[NiBr_2(DME)]$ with the corresponding Schiff-base ligands in dichloromethane at room temperature. All three complexes are red–brown powders.

In order to define the coordination mode of these α-diimine ligands, small area X-ray photoelectron spectroscopy of $NiBr_2$, free ligand $[(4\text{-Br-}2,6\text{-Me})_2DABMe_2]$, and its corresponding complex have been studied (Fig. 1). The binding energy of $Ni_{2p3/2}$ of the complex is 0.01 eV lower than with that of $NiBr_2$. This clearly shows an increase in the election density at Ni and therefore coordination of Ni with N in **$[NiBr_2(L1)]$**. Compared with **L1**, the increase (1.06 eV) in binding energy of $N_{1s1/2}$ in the complex provides further evidence for the coordination of Ni to N.

Suitable crystals of **L1** for X-ray diffraction were obtained by layering a solution of the ligand in CH_2Cl_2 with pentane. The molecular structure of **L1** was determined and the corresponding diagram is shown in Fig. 2, while selected bond distances and angles are summarized

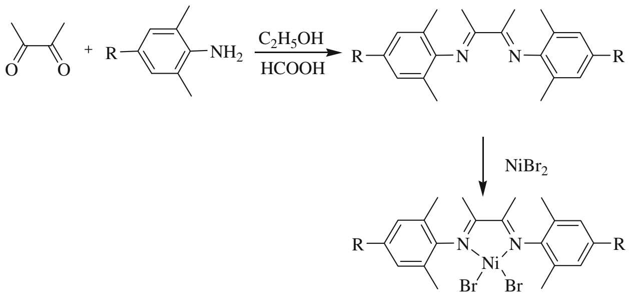

Scheme 1 Synthetic routes of the α-diimine ligands (**L1**: R=Br, **L2**: R=CH_3; **L3**: R=H) and their nickel (II) complexes (**[L1NiBr$_2$]**, **[L2NiBr$_2$]**, **[L3NiBr$_2$]**)

in Table 2. The X-ray structure of **L1** exhibits *trans*-conformation about the central C–C bond of the ligand backbone. In the solid state, the most interesting feature of this asymmetric ligand is the conformation of the substituents attached to N(1) and N(1A). These groups are rotated about 180° from the position they must occupy to chelate the metal. Bond lengths and angles are within the expected range for α-diimines; for example, the bond distances for the C(8)=N(1) double bond and the central C(8)–C(8A) single bond are 1.282(7) Å and 1.517(11) Å, which are very close to the values for other structurally characterized free α-diimines [27]. Both C(4) and C(8) possess essentially rather planar geometry (sp^2 character), as shown by the N=C–C angles, which are very close to 120°. The shortest C–H…π contact has a H …π distance of 0.9300 Å and C–H …π angle of 120°.

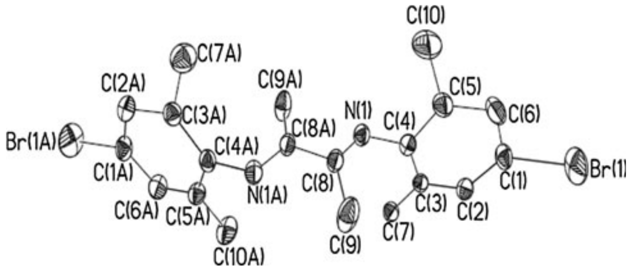

Fig. 2 ORTEP drawing of α-diimine ligand **L1** with 30% probability displacement ellipsoid (the hydrogen atoms are omitted for clarity)

Effect of ligand structure on catalyst activity and polymer properties

On treatment with DEAC, all the nickel complexes are highly active toward ethylene polymerization. The results of the polymerization experiments are shown in Table 3. In order to investigate the effect of ligand structure on the performance of the nickel catalysts, three catalysts (*para*-Br **[NiBr$_2$(L1)]**, *para*-methyl **[NiBr$_2$(L2)],** and *para*-H **[NiBr$_2$(L3)]**) were screened. Table 3 shows that the replacement of the *para*-aryl proton in **L3** by an electron-withdrawing

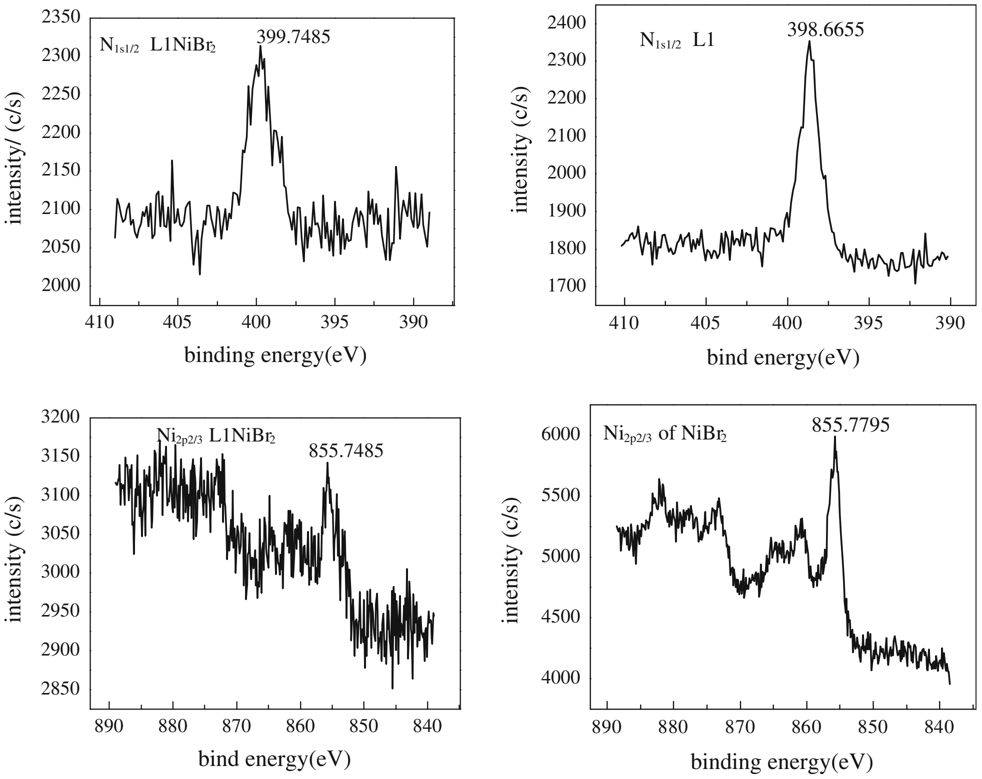

Fig. 1 XPS spectra of NiBr$_2$, **L1** and **[L1NiBr$_2$]**

Table 2 Selected bond lengths [Å] and angles [deg] for α-diimine ligand **L1**

Bond (lengths)	(Å)	Bond (angles)	(°)
Br(1)–C(1)	1.897(6)	C(6)–C(1)–C(2)	120.9(6)
C(1)–C(2)	1.384(9)	C(2)–C(1)–Br(1)	119.6(5)
C(4)–N(1)	1.428(7)	C(6)–C(1)–Br(1)	119.5(5)
C(8)–N(1)	1.282(7)	C(5)–C(4)–N(1)	117.3(6)
C(1)–C(6)	1.368(9)	N(1)–C(8)–C(8A)	115.2(7)
C(2)–C(3)	1.389(8)	N(1)–C(8)–C(9)	126.3(5)
C(5)–C(10)	1.519(10)	C(3)–C(4)–N(1)	121.0(5)
C(8)–C(8A)	1.517(11)	C(8)–N(1)–C(4)	120.4(5)

Br in **L1** results in an increase in both catalyst activity and the average molecular weight (Mw) of the polymers obtained (Entries 1 and 2 in Table 3). However, the activity of the catalyst with an electron-donating methyl group on the para-position (**L2**) is decreased (enteries 1 and 3). We conclude that the electron-withdrawing group strengthens the electrophilic character of the nickel, which increases the rate of chain propagation relative to chain transfer, leading to the increase in the molecular weight of the polyethylenes obtained. From these observations [3], the polymer Mw is the result of complex interplay between monomer insertion, chain transfer, and potential catalyst decomposition. Interestingly, the variation in the para-substituents of these α-diimine ligands has a pronounced effect not only on catalyst activity and the molecular weight but also on the degree of branching of the resulting polymer. Thus, when an electron-withdrawing substituent is introduced into the *para*-position of the 2,6-dialkylaryl imine group, the branching degree of the polyethylenes increases. It is possible that the substitution of electron-donating groups could decrease the favorability of C–H activation by perturbing the ligand geometry to limit the close approach of the metal to the ligand axial alkyl moieties.

Influence of polymerization temperature

Polymerization temperature has a great influence on the catalyst activity, as well as on polymer branching and molecular weights. Table 3 shows that the catalytic activity and molecular weight of the polyethylene produced by all three catalysts decreased as the temperature was increased. This reveals that the chain transfer increases at high temperature, although catalyst decomposition may also affect catalytic activity and molecular weight. The distribution of molecular weights was also observed to increase as the reaction temperature was increased. In addition, the branching numbers increased dramatically with increasing temperature (Table 3), indicating that the chain walking increases dramatically at high reaction temperature. The type and amount of branches formed during ethylene polymerization depended mainly on the reaction temperature but also varied with the ethylene pressure and catalyst structure. Ni(II)-α-diimine catalysts are known to produce more branches at high temperature and low ethylene pressure. As show in Table 3, the **[NiBr$_2$(L1)]**/DEAC catalytic system containing an electron-withdrawing Br group generated the highest degree of branching of polyethylene at 40 °C. The branching degree of polyethylene prepared with catalyst was 125 branches per 1,000, while the values for **[NiBr$_2$(L1)]**, **[NiBr$_2$(L2)],** and **[NiBr$_2$(L3)]** were 107.3 and 113.2 branches per 1,000 °C, respectively. Thus, the catalyst containing an electron-withdrawing group favors chain walking.

Table 3 The results of polymerization with the nickel complexes

Entry	Precatalyst	Yield (g)	Temp (°C)	Activity[b]	Mw[c] (kg/mol)	M_w/M_n^c	Branches[d] (per 1,000 °C)
1	[L1NiBr$_2$]	1.4936	0	7.47	220.9	1.79	58.3
2	[L2NiBr$_2$]	1.2826	0	6.41	207.5	1.69	39.2
3	[L3NiBr$_2$]	1.3551	0	6.78	218.0	1.61	47.6
4	[L1NiBr$_2$]	1.0653	20	5.33	187.2	1.84	89.2
5	[L2NiBr$_2$]	0.7652	20	3.83	136.0	1.82	70.7
6	[L3NiBr$_2$]	0.8080	20	4.04	155.4	1.65	76.9
7	[L1NiBr$_2$]	0.6544	40	3.27	83.9	2.06	125
8	[L2NiBr$_2$]	0.4823	40	2.41	50.5	1.93	107.3
9	[L3NiBr$_2$]	0.5568	40	2.78	66.5	1.69	113.2

[a] Polymerization condition: 2 μmol precatalyst, Al/Ni = 600 (molar ratio), polymerization reaction under 0.02 Mpa for 30 min

[b] {$\times 10^6$ g PE/(molNi.h.Bar)}

[c] Weight-average molecular weight and polydispersity index determined by GPC

[d] Degree of branching determined by ^{1}H NMR

Figure 3 summarizes the ^{13}C NMR spectra of the polymers prepared with the three catalysts at 40 °C. The ^{13}C NMR spectra (Fig. 3) of the polyethylenes prepared at 40 °C exhibited resonances at 19.60, 27.41, and 33.32 ppm due to the methyl branch carbon. Ethyl branch was identified by the presence of resonances at 11.20 and 37.10 ppm, while the resonance at 22.71 ppm corresponds to the butyl branch carbon [28]. From the resonance intensities of Fig. 3, the main branch is methyl.

Figure 4 shows the ^{1}H NMR spectra of the polymers prepared with the three catalysts at 40 °C. The doublets at 0.86 ppm were assigned to the methyl group, those at 1.15 ppm to the methylene group, and the broad resonances at 1.28 ppm to the methine group. The resonances of the methyl group are split into doublets due to the methyl branch. However, the small shoulder resonances at 0.98 ppm suggest the presence of other longer branches. This is consistent with ^{13}C NMR analysis.

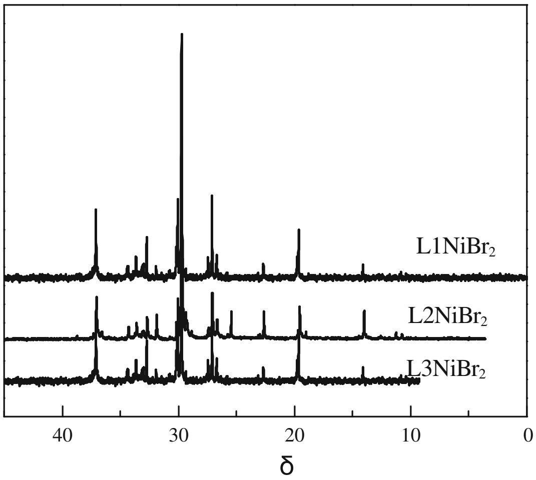

Fig. 3 ^{13}C NMR spectra of polyethylene obtained from at 40 °C **[L1NiBr$_2$]** run 7, **[L2NiBr$_2$]** run 8 and **[L3NiBr$_2$]** run 9

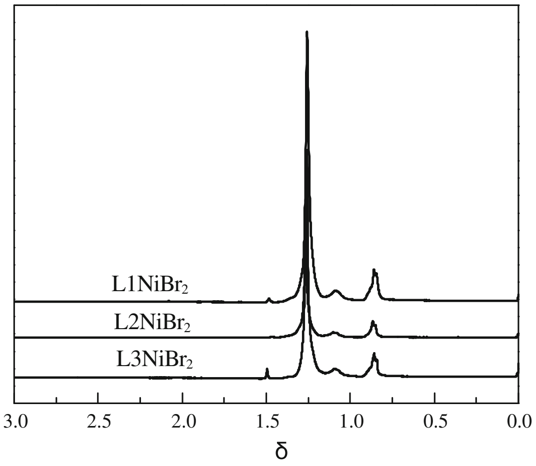

Fig. 4 ^{1}H NMR spectra of polyethylene prepared with catalysts/DEAC at 40 °C (1) run 7, (2) run 8 and (3) run 9

Conclusion

A new α-diimine ligand **L1** bearing an electron-withdrawing Br group and its Ni(II) complex have been prepared and characterized. **L1** was also modified in an attempt to change the electronic density of the metal center and so to improve the activity of the catalyst, the molecular weight, and the branching degree of polyethylene produced. In comparison with the non-brominated α-diimine nickel complexes, the complex **[NiBr$_2$(L1)]**, activated by DEAC, showed high activity and produced high molecular weight and branching of the polymer. Investigations into the copolymerization catalysis of the α-diimine nickel complexes are now in progress.

Acknowledgments The research was financially supported by NSFC (20964003). We also thank Key Laboratory of Eco-Environment-Related Polymer Materials (Northwest Normal University), Ministry of Education, for financial support.

References

1. Johnson LK, Killian CM, Brookhart M (1995) J Am Chem Soc 117:6414
2. Ittel SD, Johnson LK, Brookhart M (2000) Chem Rev 100:1169
3. Camacho DH, Guan ZB (2010) Chem Commun 46:7879
4. Killian CM, Johnson LK, Brookhart M (1997) Organometallics 16:2005
5. Choi Y, Soares João BP (2010) Polymer 51:2271
6. Gates DP, Svejda SA, Oate E, Killian CM, Johnson LK, White PS, Brookhart M (2000) Macromolecules 33:2320
7. Popeney CS, Rheingold AL, Guan ZB (2009) Organometallics 28:4452
8. Liu FS, Hu HB, Xu Y, Guo LH, Zai SB, Song KM, Gao HY, Zhang L, Zhu FM, Wu Q (2009) Macromolecules 42:7789
9. Mecking S, Johnson LK, Wang L, Brookhart M (1998) J Am Chem Soc 120:888
10. Camacho DH, Salo EV, Ziller JW, Guan ZB (2004) Angew Chem Int Ed 43:1821
11. Gottker-Schnetmann I, Korthals B, Mecking S (2006) J Am Chem Soc 128:7708
12. Luo S, Vela J, Lief GR, Jordan RF (2007) J Am Chem Soc 129:8946
13. Helldorfer M, Backhaus J, Milius W, Alt HG (2003) J Mol Catal A Chem 193:59
14. Helldorfer M, Milius W, Alt HG (2003) J Mol Catal A Chem 197:1
15. Zhang TZ, Guo DW, Jie SY, Sun WH, Li T, Yang XZ (2004) J Polym Sci Part A Polym Chem 42:4765
16. Popeney CS, Guan ZB (2005) Organometallics 24:1145
17. Helldorfer M, Backhaus J, Alt HG (2003) Alt Inorganica Chimica Acta 351:34
18. Kravchenko R, Waymouth RM (1997) Macromolecules 30:1

19. Schneider MJ, Mulhanupt R (1997) Macromol Chem Phys 198:883
20. Jin J, Uozumi T, Sano T, Teranishi T, Soga K, Shiono T (1998) Macromol Rapid Commun 19:337
21. Shiono T, Moriki Y, Soga K (1995) Macromol Symp 97:161
22. Malmberg A, Kokko E, Lehmus P, Lofgren B, Seppala JV (1998) Macromolecules 31:8448
23. Wang WJ, Yanh D, Zhu S, Hamielec AE (1998) Macromolecules 31:8677
24. Yuan JC, Silva LC, Gomes PT, Valerga P, Campos TM, Ribeiro MR, Chien JCW, Marques MM (2005) Polymer 46:2122
25. Liu HR, Gomes PT, Costa SI, Duarte MT, Branquinho R, Fernandes AC, Chien JCW, Singh RP, Marques MM (2005) Organomet Chem 690:1314
26. Ward LGL, Pipal JR (1972) Inorg Synt 13:162
27. Van KG, Vrieze K (1982) Adv Organomet Chem 21:151
28. Linderman LP, Adams NO (1971) Anal Chem 43:12